

Towards the First DRESDYN Precession Experiments

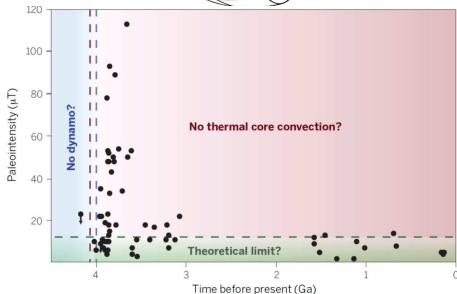
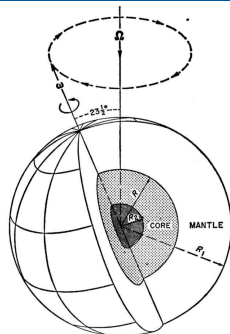
André Giesecke

Helmholtz-Zentrum Dresden-Rossendorf

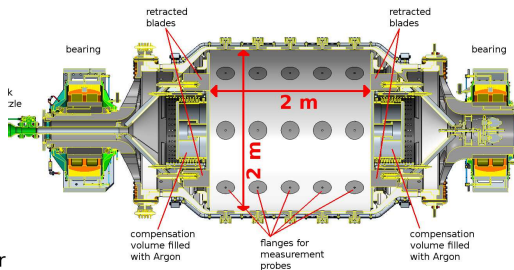
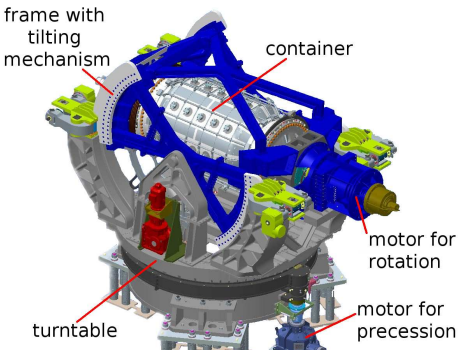
ASTROMHD@HZDR
Dresden, March 19, 2019

Motivation for precession dynamo

- alternative dynamo concept: **mechanical forcing**
 - ⇒ **efficient flow driving on lab scale**
 - ⇒ no propellers or pumps
 - ⇒ “natural” mechanism
- may be relevant for planets/moons
 - ⇒ **geodynamo** (Malkus 1968)
 - ⇒ **ancient lunar dynamo** (Weiss 2014)
- precession driven dynamos have been **found in simulations** (Tilgner 2005, Wu & Roberts 2009, Nore 2011)
- experiments by Gans (1971) show **field-amplification** by factor of 3 in small precessing cylinder with $R = 0.125$ m and $\nu_c = 60$ Hz



Design parameters of the precession dynamo



currently under construction
first run planned for 2019

rotation rate	precession rate	nutaton angle	Reynolds	magnetic Reynolds	aspect ratio	precession ratio
$f_c = \frac{\Omega_c}{2\pi}$	$f_p = \frac{\Omega_p}{2\pi}$	α	$Re = \frac{\Omega_c R^2}{\nu}$	$Rm = \frac{\Omega_c R^2}{\eta}$	$\Gamma = \frac{H}{R}$	$Po = \frac{\Omega_p}{\Omega_c}$
0 ... 10 Hz	0 ... 1 Hz	45° ... 90°	up to 10 ⁸	up to 700	2	0 ... 0.1

Characterisation of flow in terms of inertial modes

Navier-Stokes in precessing frame (BC: $\mathbf{u} = \boldsymbol{\Omega}_c \times \mathbf{r}$)

$$\frac{\partial \mathbf{u}}{\partial t} + \mathbf{u} \cdot \nabla \mathbf{u} + 2\boldsymbol{\Omega}_p \times \mathbf{u} = -\nabla P + \nu \nabla^2 \mathbf{u}$$

linear inviscid approximation $\frac{\partial \mathbf{u}}{\partial t} + 2\boldsymbol{\Omega}_p \times \mathbf{u} = -\nabla P$

- Solutions are **inertial waves** or **Kelvin modes** characterized by azimuthal, axial and “radial” wavenumber $m, k, l \rightarrow j$:

$$\mathbf{u}^j = \exp(i\omega_j t + im\varphi) \begin{pmatrix} \tilde{u}_r^j(r) \cos(\pi k z) \\ \tilde{u}_\varphi^j(r) \cos(\pi k z) \\ \tilde{u}_z^j(r) \sin(\pi k z) \end{pmatrix} + c.c$$

- **Kelvin modes** are eigenfunctions of the linearized inviscid Navier-Stokes equation for rotating fluids in cylindrical geometry which satisfy free-slip boundary conditions

Structure of Kelvin modes

- frequency ω_j obtained from **dispersion relation**:

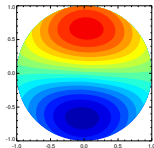
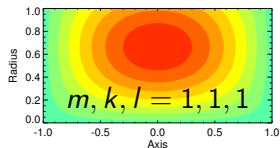
$$\omega_j = \pm 2\sqrt{\left(1 + \left(\frac{\lambda_j}{k\pi}\right)^2\right)^{-1}} \quad \text{with } \omega_j \lambda_j J_{m-1}(\lambda_j) + m(2 - \omega_j) J_m(\lambda_j) = 0$$

$$u_r^j = \left[\frac{-i}{4 - \omega_j^2} \right] \left[\omega_j \lambda_j J_{m-1}(\lambda_j r) + \frac{m(2 - \omega_j)}{r} J_m(\lambda_j r) \right] \cos(k\pi z)$$

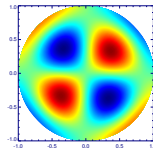
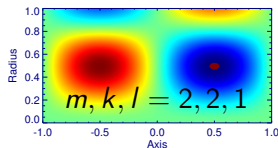
$$u_\varphi^j = \left[\frac{1}{4 - \omega_j^2} \right] \left[2\lambda_j J_{m-1}(\lambda_j r) - \frac{m(2 - \omega_j)}{r} J_m(\lambda_j r) \right] \cos(k\pi z)$$

$$u_z^j = -i \frac{k\pi}{\omega_j} J_m(\lambda_j r) \sin(k\pi z) \quad \mathbf{j = m, k, l}$$

axial velocity u_z

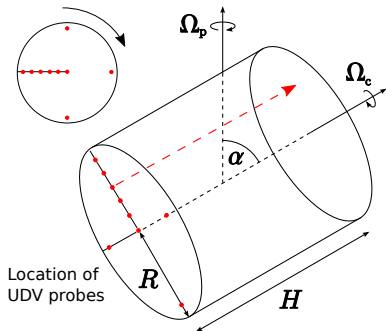
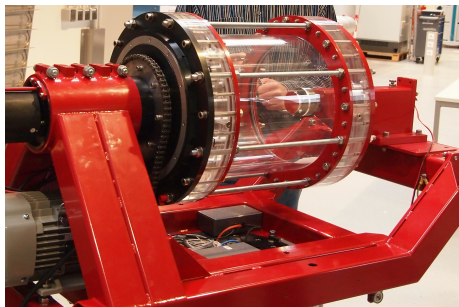


axial velocity u_z



Hydrodynamics of precession driven flows

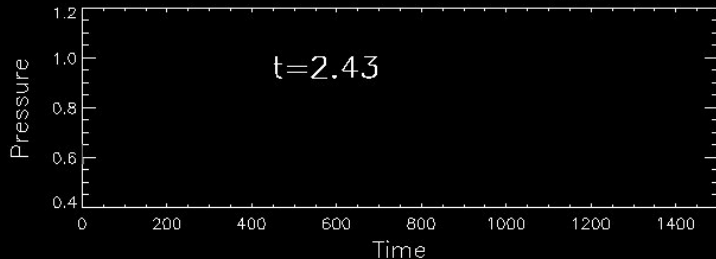
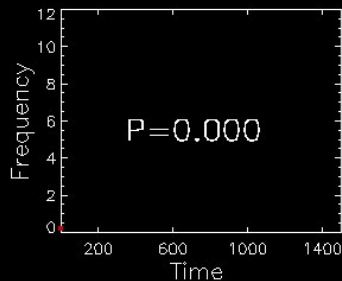
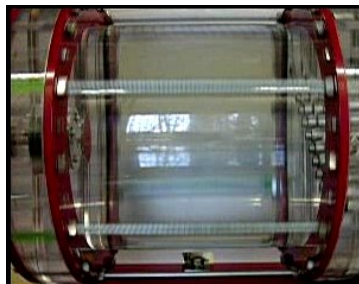
- numerical simulations with **SEMTEX** (Blackburn & Sherwin 2004)
- flow measurements with UDV at model water experiment ($R = 0.163$ m)



aspect ratio	$\Gamma = H/R = 2$	precession ratio	$Po = \Omega_p / \Omega_c $	$0 \dots 0.1$
precession angle	$\alpha = 90^\circ$ ($\Omega_p \perp \Omega_c$)	Reynolds number	$Re = \Omega_c R^2/\nu$	$10^4 \dots 10^6$

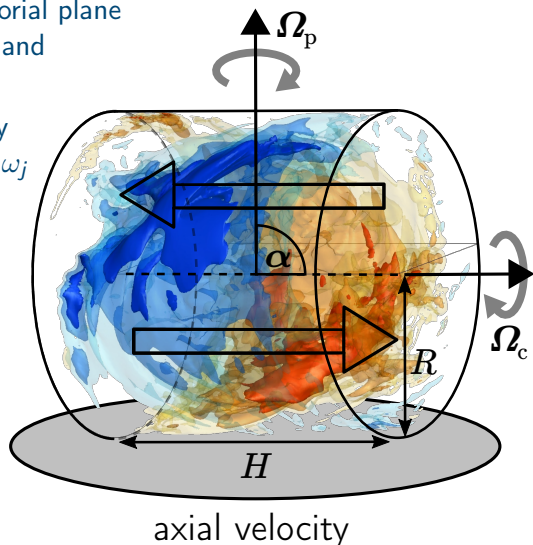
- **structure**, **amplitude**, time-dependent features (e.g. free inertial waves)
- $Re = 10^4 \Rightarrow$ **lower limit of motor = upper limit of simulations**

The water precession experiment

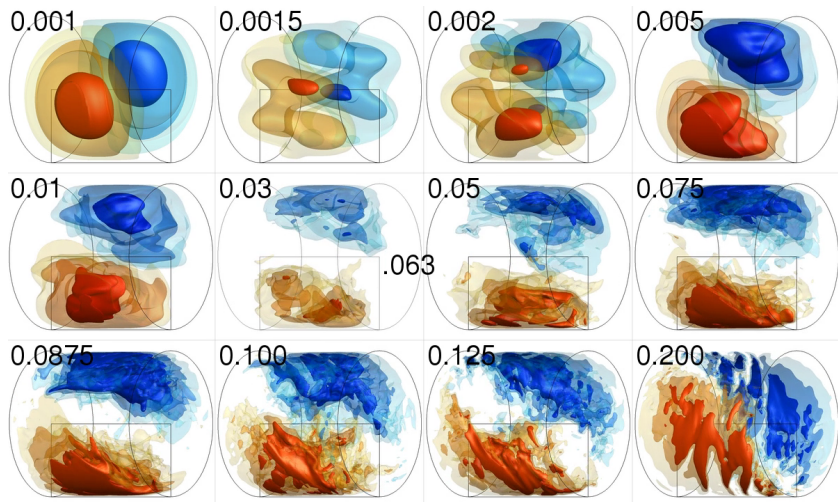


The forced mode in simulations

- **structure of forcing** $F_p = -\Omega_p \Omega_c r \sin \alpha \cos(\Omega_c t + \varphi)$
 - ⇒ antisymmetric w.r.t. equatorial plane
 - ⇒ inertial modes with $m = 1$ and k odd are directly forced
- **resonance** if forcing frequency Ω_c is equal to eigenfrequency ω_j
 - ⇒ mode $(m, k, \omega) = (1, 1, 1)$ is **resonant** at $\Gamma = 1.98982$
- **non-linear self-interaction** forbidden at 1st order (Greenspan 1969) but
 - $(m, k, \omega) \rightarrow (2m, 2k, 2\omega)$
 - $(m, k, \omega) \rightarrow (0, 2k, 0)$
 - $(m, k, \omega) \rightarrow (0, 0, 0)$observed in **simulations** and **experiments**

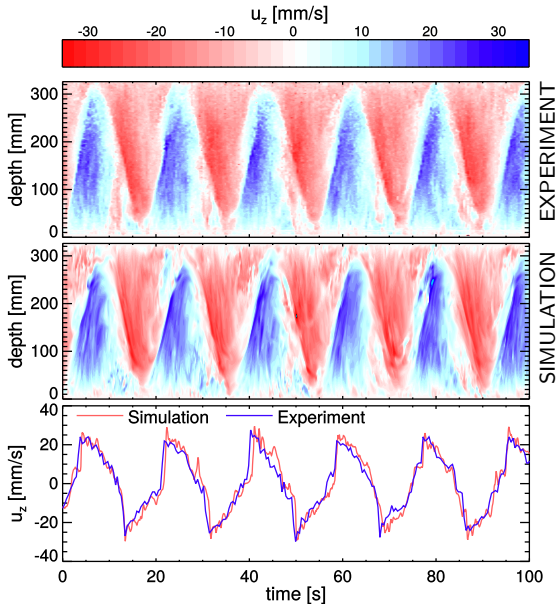


Flow structure in simulations



u_z in trnstable system for increasing Po (from $Po = 0.001$ to $Po = 0.2$)

Comparison with experiment: Flow structure



- axial profiles of u_z at $r = 150$ mm in co-rotating frame
- superposition of $m = 1$, multiples and axisymmetric flow
- excellent agreement between simulations and experiment
- validation restricted to $Re = 10^4$ (corresponding to $\nu_c = 0.06$ Hz)

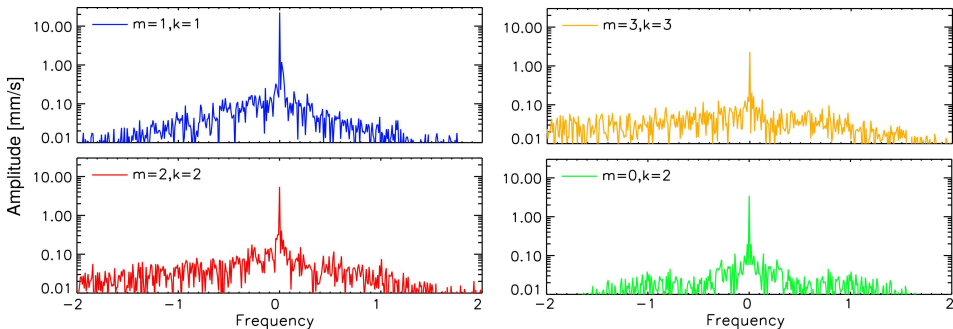
Spectra from simulations ($\text{Re} = 10^4$ and $\text{Po} = 0.1$)

$$\tilde{u}_z^k(r, \varphi_j, t_n) = \frac{1}{N_z} \sum_{l=1}^{N_z} u_z(r, \varphi_j, z_l, t_n) \sin\left(\frac{k\pi z_l}{H}\right)$$

axial mode at
timestep t_n

$$\tilde{\tilde{u}}_z^k(r, m, \omega) = \frac{1}{N_\varphi N_t} \sum_{n=1}^{N_t} \sum_{j=1}^{N_\varphi} \tilde{u}_z^k(r, \varphi_j, t_n) e^{-i(m\varphi_j + \omega t_n)}$$

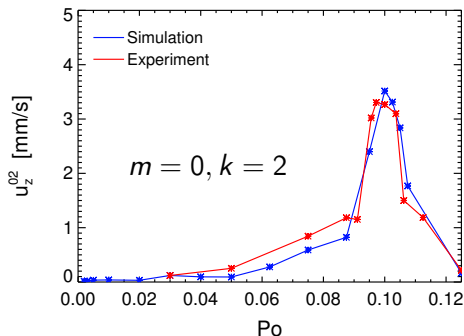
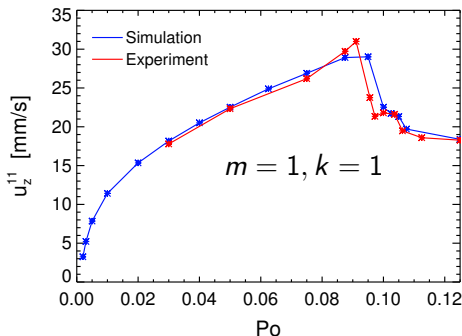
2D FFT in
 φ and t



■ flow dominated by standing inertial waves

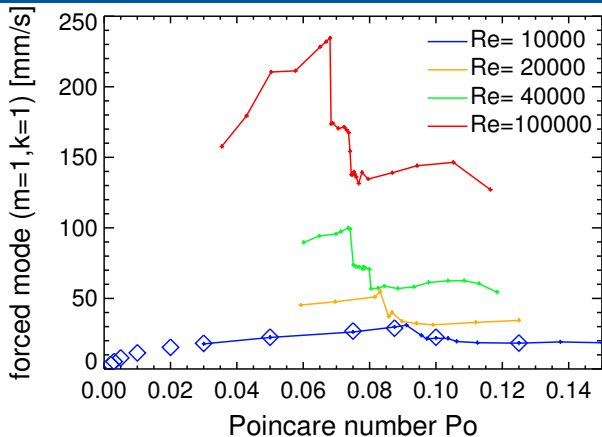
Comparison with experiment: Amplitudes

- 'projection' on Kelvin mode $\propto \sin(kz) \cos(m\varphi)$ at fixed r
 \Rightarrow **time-independent** contributions dominate



- maximum of forced Kelvin mode around $Po \approx 0.09$
- emergence of axisymmetric mode with $k = 2$ in the range $0.095 < Po < 0.105$

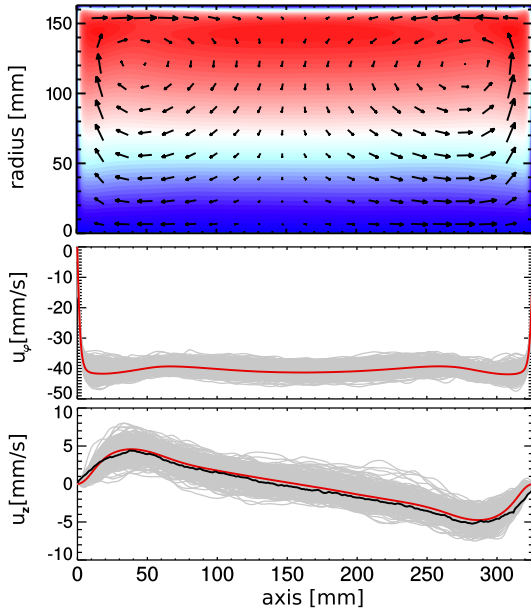
Amplitudes for increasing Re (Experiment)



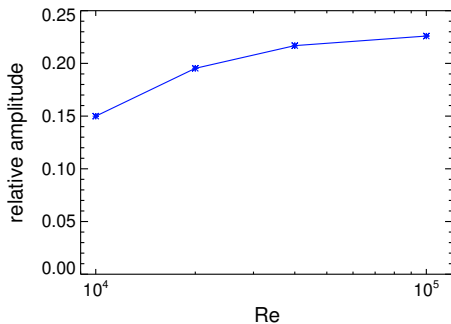
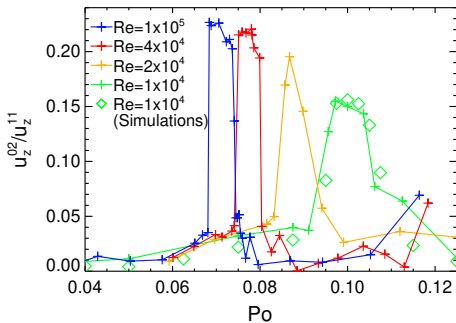
- abrupt breakdown of $m = 1$ above critical precession ratio Po^{crit} with Po^{crit} decreasing when Re increases
- decrease describes a two-stage process with an intermediate plateau with width $\Delta Po \approx 0.006$

Pattern of axisymmetric flow

- meridional axisymmetric flow (u_r, u_z) with $m = 0, k = 2$
- double roll structure similar to mean flow in VKS dynamo
- toroidal flow (u_φ^{m0}) is composed of boundary layer and geostrophic part with $k = 0$ (braking of SBR)
- comparison with measurements (black curve) show good agreement for time-averaged flow u_z

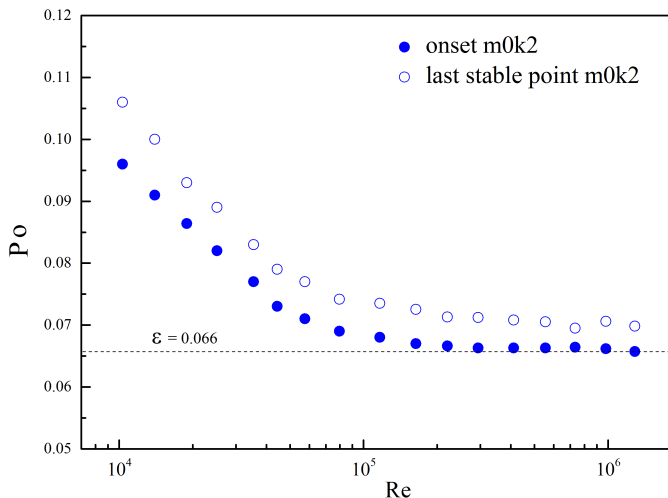


Evolution for increasing Reynolds number



- resonant-like appearance of axisymmetric mode
- Po^{crit} for appearance of $m=0$ mode decreases for increasing Re
- $m=0$ mode becomes more important for increasing Re
- width of regime with $m=0$ mode only weakly affected

Scaling to the large scale experiment

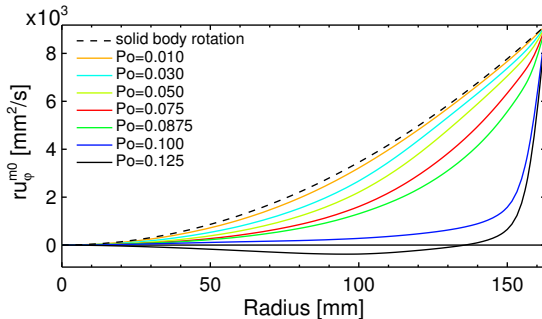
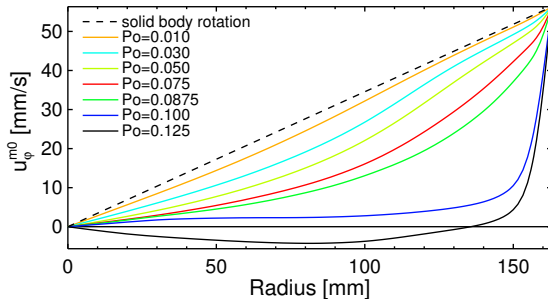


- location of regime with $m = 0$ mode varies linearly until $Re \sim 10^5$
- asymptotic behavior with $Po^{crit} \approx 0.066$ for $Re > 10^5$

Circulation flow (axisymmetric azimuthal flow)

- strong impact of precession on initial solid body rotation
- ⇒ “braking” of bulk flow
- mean flow generation from nonlinear self-interaction of directly forced flow?
- strong gradient (shear) close to outer boundary
- violation of **Rayleigh criteria** for stability of rotating fluids

$$\frac{d}{dr}(ru_{\varphi}^{m0}) < 0$$



The dynamo problem

compute numerical solution of induction equation

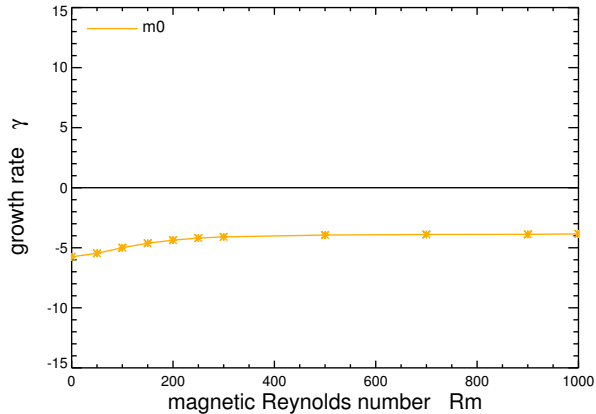
$$\frac{\partial \mathbf{B}}{\partial t} = \nabla \times (\mathbf{u} \times \mathbf{B} - \eta \nabla \times \mathbf{B})$$

- ⇒ **growth rates** and **critical magnetic Reynolds number**
- ⇒ structure of magnetic field close to onset of dynamo action

Numerical approach

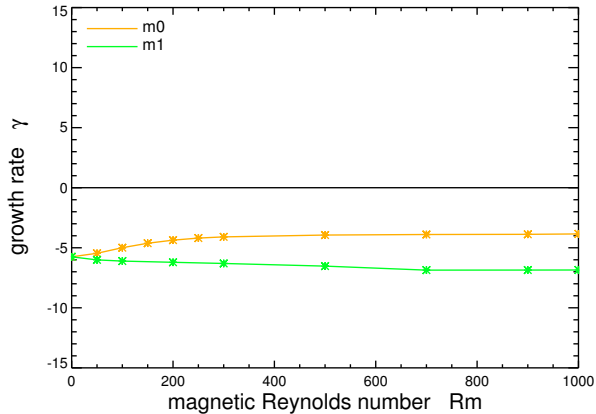
- consider kinematic problem with **prescribed velocity field**
 - ⇒ **time-averaged** velocity-field from hydro simulations
- impact of largest azimuthal velocity modes ($m = 0, 1, 2, 3, \dots$)
- **no backreaction**, no **time-dependent** fluctuations
- **pseudo vacuum** boundary conditions for magnetic field

Dynamos with time-averaged flow: Impact of m_0 flow



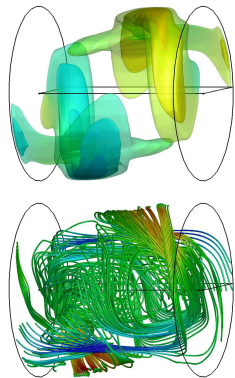
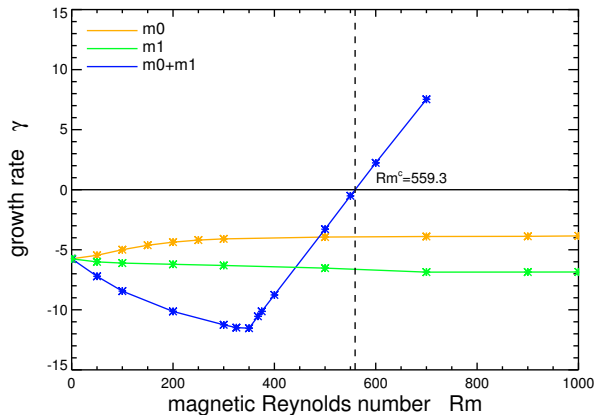
■ no dynamo from axisymmetric flow

Dynamos with time-averaged flow: Impact of m_0 flow



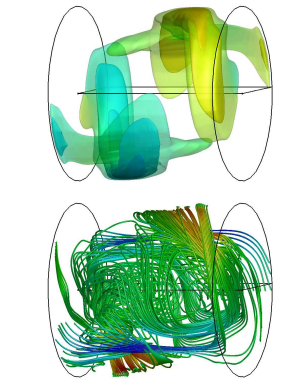
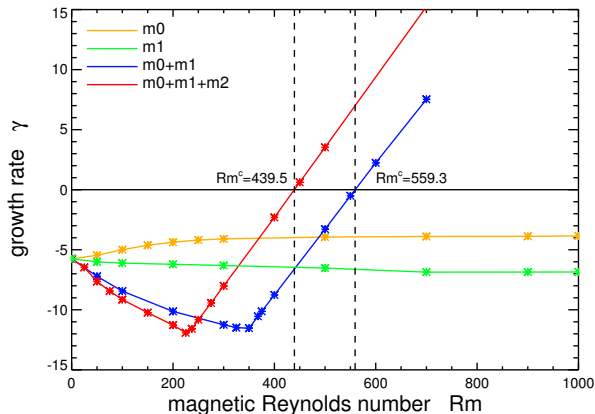
■ no dynamo from axisymmetric flow or $m = 1$ flow

Dynamos with time-averaged flow: Impact of m_0 flow



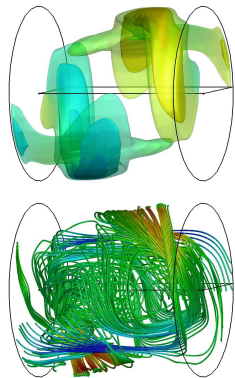
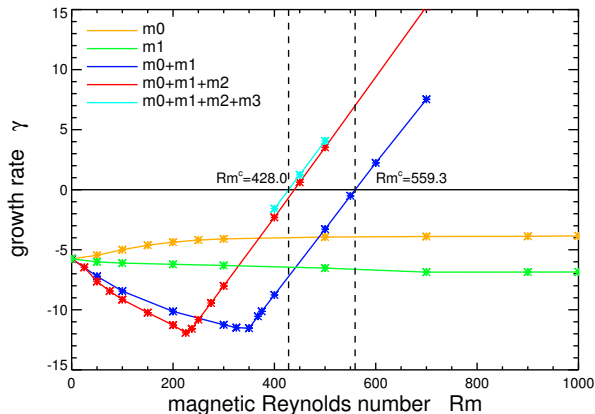
- **no dynamo** from axisymmetric flow or $m = 1$ flow
- combination of axisym. flow and $m = 1$ gives **dynamo at $Rm^c \approx 560$**

Dynamos with time-averaged flow: Impact of m_0 flow



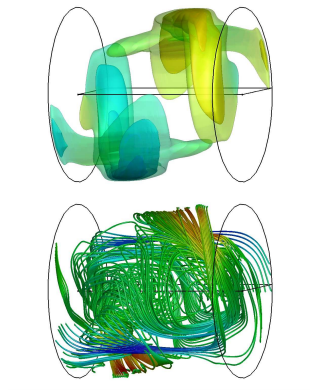
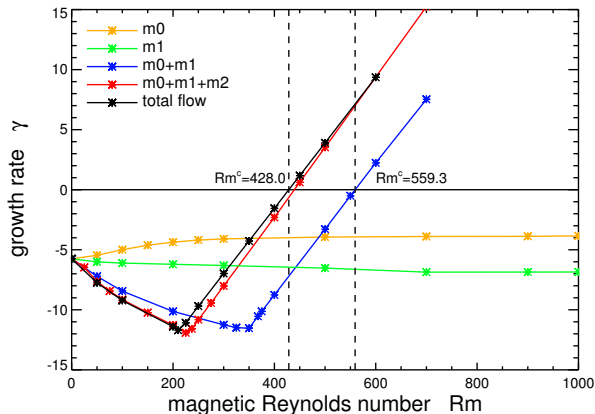
- **no dynamo** from axisymmetric flow or $m = 1$ flow
- combination of axisym. flow and $m = 1$ gives **dynamo at $Rm^c \approx 560$**
- contributions that increase **parity breaking** improve dynamo action
 \Rightarrow reduction to **$Rm^c \approx 430$** when $m = 2$ and/or $m = 3$ are added

Dynamos with time-averaged flow: Impact of m_0 flow



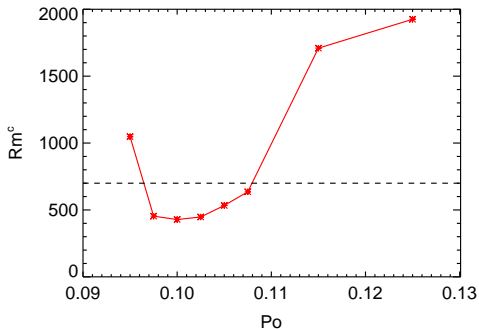
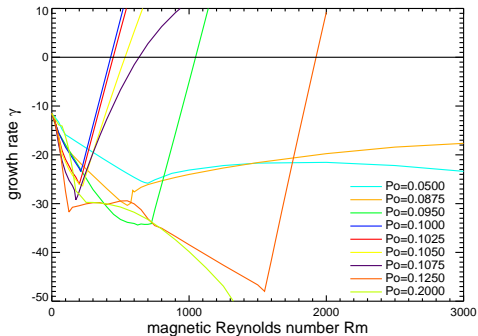
- no dynamo from axisymmetric flow or $m = 1$ flow
- combination of axisym. flow and $m = 1$ gives dynamo at $Rm^c \approx 560$
- contributions that increase parity breaking improve dynamo action
⇒ reduction to $Rm^c \approx 430$ when $m = 2$ and/or $m = 3$ are added

Dynamos with time-averaged flow: Impact of m_0 flow



- no dynamo from axisymmetric flow or $m = 1$ flow
- combination of axisym. flow and $m = 1$ gives dynamo at $Rm^c \approx 560$
- contributions that increase parity breaking improve dynamo action
 \Rightarrow reduction to $Rm^c \approx 430$ when $m = 2$ and/or $m = 3$ are added

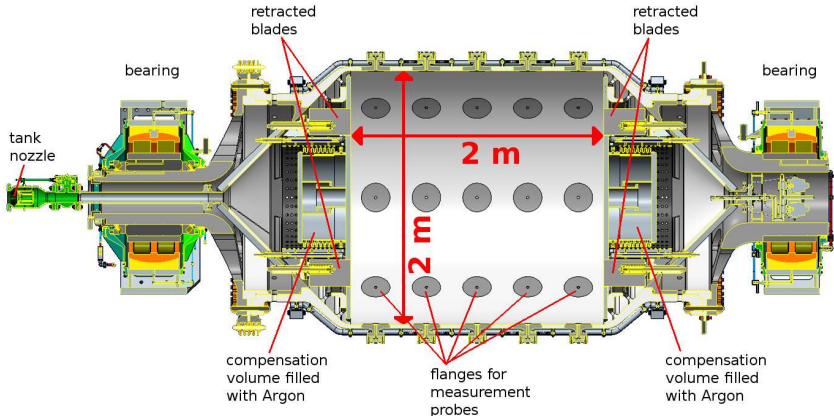
Kinematic Dynamos with time-averaged flow II: total flow



- only flow fields computed from hydrodynamic simulations above $Po = 0.095$ exhibit dynamo action
- without the axisymmetric flow we do not find dynamo action
- Rm^{crit} sufficiently small (i.e. experimentally accessible) for flow fields with $Po \in [0.0975, 0.1075]$.

Characterization of flow state in the large experiment

- direct flow measurements with UDV will be difficult (not possible?)
- global quantities: **power consumption, slip, torque (wish)**
- local measurements: **pressure (at wall), magnetic fields (future topic)**



Power consumption and torque

Power P is related to torque Γ via angular velocity Ω according to $P = \Gamma \Omega$

- simplest assumption (see e.g. VKS, Mordant et al 1997, J. Phys. II France, 7 (11), 1729–1742, DOI: 0.1051/jp2:1997212): mean torque scales according to

$$\Gamma = \rho R^5 \Omega^2 f(\text{Re})$$

with f an unknown function of $\text{Re} = R^2 \Omega / \nu$ that depends on the way energy is injected into the flow

- express torque in terms of internal flow variables $\Gamma \sim u_{\text{rms}}^2$, to be estimated from global measurements, e.g., $u_{\text{rms}} \sim \sqrt{p_{\text{rms}}}$
- u_{rms} characterizes flow behavior in the bulk, whereas p_{rms} is taken from measurements of the pressure at the wall
- example VKS: laminar regime $f(\text{Re}) \sim \text{Re}^{-1/2}$ whereas in turbulent regime $f(\text{Re}) \sim \text{Re}^{-1/5}$ (turbulent boundary layers, Schlichting)
- probably different in precession case where power injection occurs mainly via pressure forces in corners

Estimation of internal losses

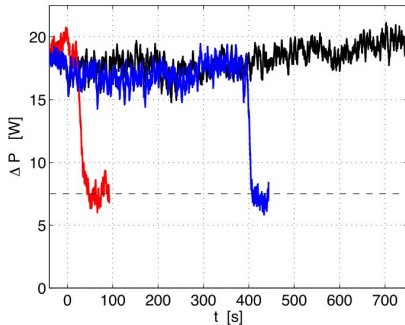
- instantaneous power consumption of an equilibrated motor

$$P(t) = \frac{\sqrt{3}}{2} U(t) I(t) \cos \left(\varphi(t) + \frac{\pi}{6} \right) - \frac{3}{4} R_I I(t)^2$$

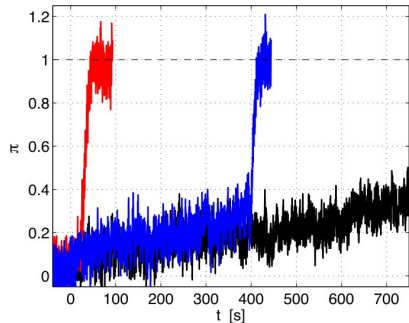
- measure $U(t), I(t), \varphi(t), R_I$
- problem: power consumption of motor $P(t)$ comprises power dissipated by the flow P_f (required) and internal mechanical and electromagnetic losses P_{lo} (unknown)
- estimation of internal losses via measurements of P without precession show scaling $P_{lo} \sim \Omega_c^2$

Example for power consumption and wall pressure

- Power consumption vs time and rescaled pressure vs time for decrease of $Po = 0.085$ (turbulent regime) to $Po = 0.0684$ (nonlinear regime)



Power consumption

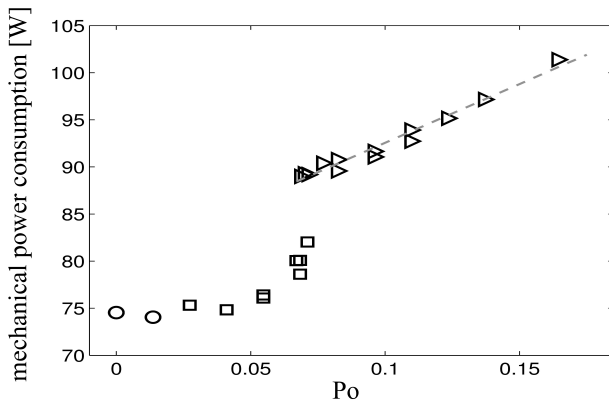


Wall pressure

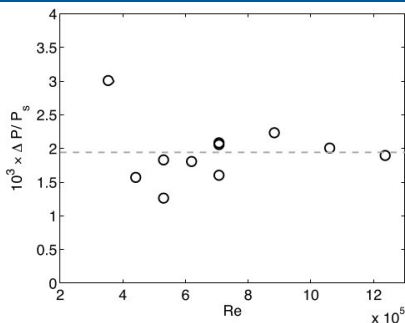
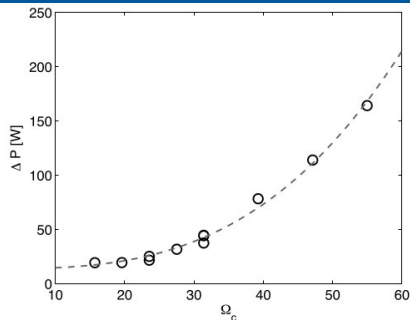
Transition from linear to turbulent state

- laminar regime with no variation with P_o
- nonlinear regime with rapid increase of P_m
- turbulent regimes with linear increase (at fixed Re)

$$P_f = P_f^0 + CP_o$$



Scaling and open questions



measurements

viscous linear theory

upper bound estimation

$$\frac{P_f}{\rho R^5 \Omega_c^3} \sim Po$$

$$\frac{P_f}{\rho R^5 \Omega_c^3} \sim Po^2 Re$$

$$\frac{P_f}{\rho R^5 \Omega_c^3} \sim \text{const}$$

- increased internal friction from increasing gyroscoping moments acting on rotating parts \Rightarrow **internal losses are not independent of precession**
- power insertion essentially via pressure in corners, boundary layers less important \Rightarrow **different scaling**

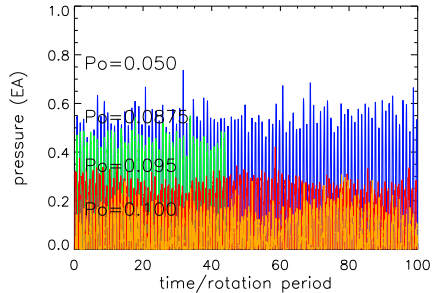
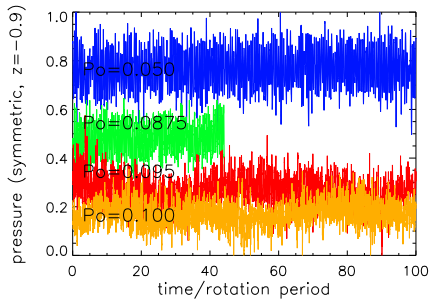
Pressure in numerical simulations

- simulations with SEMTEX make use of pressure fixed to ensure that after each timestep the velocity field is divergence free (i.e. $\nabla \cdot \mathbf{u} = 0$, incompressibility condition)
- centrifugal pressure is not considered because it doesn't cause any flow
- any constant field can be added to p without changing the results
 \Rightarrow calibration not possible without further assumptions (e.g. minimum pressure = 0)
- pressure equation:

$$\Delta p = -\rho \nabla \cdot [(\mathbf{u} \nabla) \mathbf{u}] = -\rho \frac{\partial^2 (u_i u_j)}{\partial x_i \partial x_j}$$

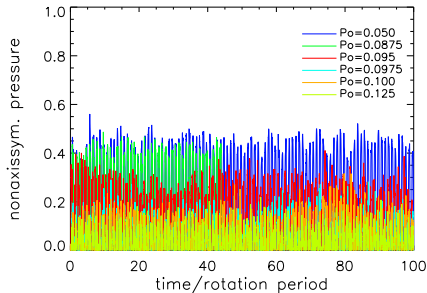
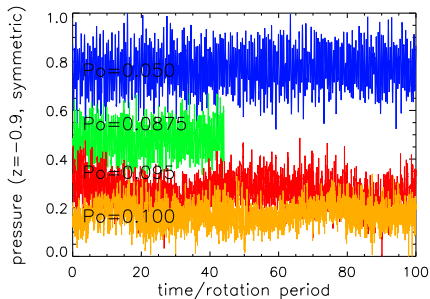
\Rightarrow involves flow gradients and motivates relation between p and u_{rms}

Pressure evolution in simulations



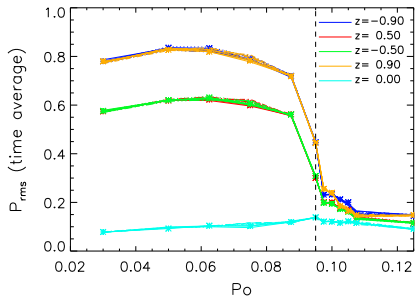
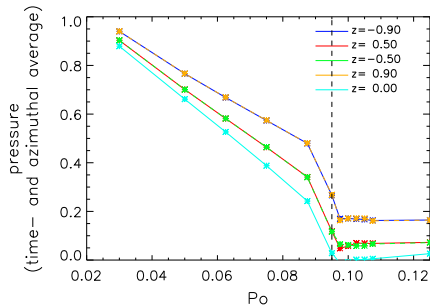
equatorially symmetric part of the pressure $P_S = (P_1 + P_2)/2$ and equatorially antisymmetric part $P_A = (P_1 - P_2)/2$ from a set of opposite (virtual) probes at $z = -0.9$ and $z = +0.9$ (and same angle)

Pressure evolution in simulations



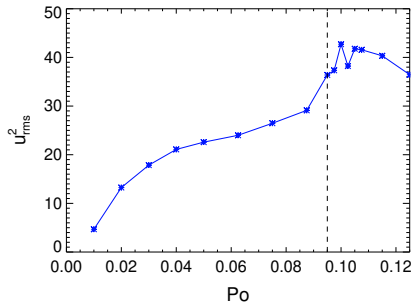
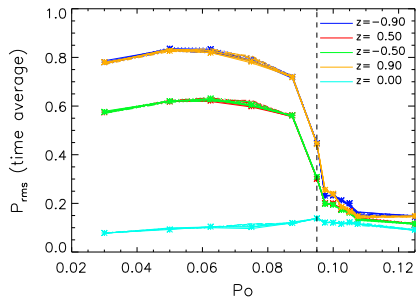
axially symmetric part of the pressure $P_S = (P_1 + P_2)/2$ and nonaxi-symmetric part $P_A = (P_1 - P_2)/2$ from a set of opposite (virtual) probes at $z = -0.9$

Pressure measurements and u_{rms}



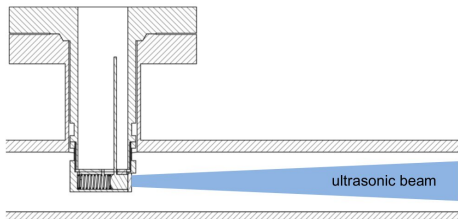
- Left: pressure measurements show linear decrease with P_0 followed by a “sharp” jump and constant behavior in the turbulent regime
 - Right: p_{rms} defined with quadratic deviation from time-averaged pressure $p_{\text{rms}} = \sqrt{\sum (p(t) - \bar{p})^2}$ exhibits qualitatively different behavior
- transition can be seen in all measurements of pressure
 - best visibility when using p_{rms} from measurements close to end caps

Comparison of p_{rms} and u_{rms}



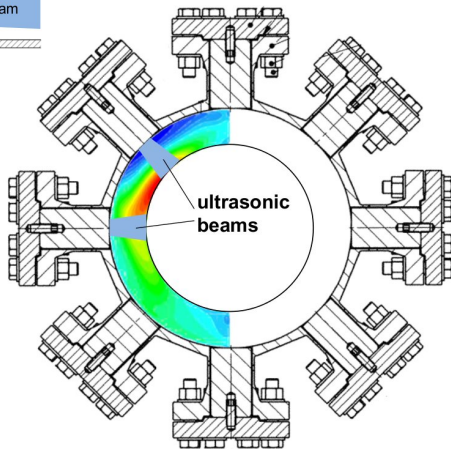
- limited agreement of comparison between p_{rms} and u_{rms}^2
- preliminary results, check calculations for u_{rms} and how to scale u_{rms}

UDV at the large precession device



- measurement of axial velocity from sensor flanges only possible close to the side wall (?)

- measurement of radial velocity at sensor flanges (6 in φ , 5 along z)
- large velocities constrain applicability (travel time of ultrasound signals, integration time, penetration depth, resolution)



Figures taken from S. Franke 2015, 'Report on the specification of the the UDV measuring concept for PEMDYN.'

UDV parameters

- UDV transducer, flow and measurement parameters for sodium at temperature $T = 150^\circ\text{C}$, $c_s = 2485\text{ m/s}$

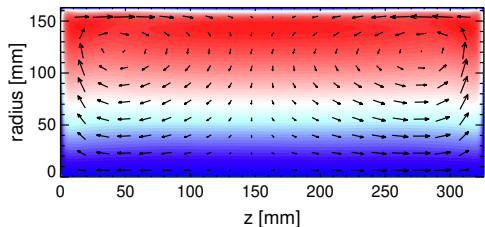
Emission frequency	max. velocity	penetration depth	axial res.	lateral res. ($z = 0.1 \dots 0.6\text{ m}$)
1 MHz	1 m/s	0.772 m	2.5 mm	26 ... 153 mm
1 MHz	2 m/s	0.386 m	2.5 mm	26 ... 153 mm
1 MHz	5 m/s	0.154 m	2.5 mm	26 ... 153 mm
1 MHz	10 m/s	0.077 m	2.5 mm	26 ... 153 mm
2 MHz	1 m/s	0.386 m	1.2 mm	13 ... 76 mm
2 MHz	2 m/s	0.193 m	1.2 mm	13 ... 76 mm
2 MHz	5 m/s	0.077 m	1.2 mm	13 ... 76 mm

- simulations and water experiments \Rightarrow typical speed in interior $\sim 30\%$ of the rotation velocity at outer rim: $u_\varphi(R = 1\text{ m})$
- $u_z^{\max} \approx 1\text{ m/s} \Rightarrow f = \frac{3\text{ m/s}}{2\pi \cdot 1\text{ m}} \approx 0.5\text{ Hz}$ ($\text{Rm} \sim 30$) for 77 cm depth

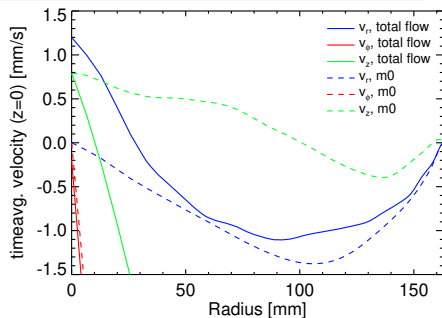
Estimations from naive scaling

timeaveraged flow in equatorial plane (mantle-frame)

- ⇒ small but 'coherent' radial $m = 0$ component $u_r(m = 0)$
- ⇒ minimal azimuthal/radial $m = 1$ component $u_{r,z}(m = 1)$
- ⇒ maximum axial $m = 1$ component $u_z(m = 1)$
- ⇒ strong azimuthal $m = 0$ component $u_\varphi(m = 0)$ (braking)



- $c_s \approx 2500 \text{ m/s} \Rightarrow \Delta t(1 \text{ m}) \approx 4 \times 10^{-4} \text{ s}$
scale to $\text{Rm} \approx 500 (f \sim 7 \text{ Hz}) \Rightarrow v_\varphi^R \sim 45$
 $\Rightarrow v_z^{m1} \sim 15 \text{ m/s}, v_\varphi^{m0} \sim 30 \text{ m/s}, v_r^{m0} \sim 1 \text{ m/s}$
 $\Rightarrow t^m \sim 0.01 \text{ s} \Rightarrow \Delta x \sim 30 \cdot 0.01 \approx 0.3 \text{ m}$



optimization \Rightarrow detection of $m = 0$ mode possible in equatorial plane?

Summary

- dynamo observed in small parameter regime in kinematic simulations using timeaveraged flow; robustness must be checked by considering impact of boundary conditions and impact of temporal fluctuations
- **pressure:**
 - flow transition should be detectable using p_{rms}
 - requires calculation of a moving average for pressure
- **Ultrasonic Doppler Velocimetry UDV:**
 - axisymmetric flow mode might be detectable qualitatively measuring the radial flow in the equatorial plane, but optimization necessary.
 - reasonable quantitative flow measurements may be possible up to $f \sim 0.5 \text{ Hz}$ (corresponding to $\text{Rm} \sim 30$)
- **power input:**
 - power input constrains available energy for flow driving
 - so far measurements are not in accordance with theory (not surprising)
 - internal losses are unknown \Rightarrow better calibration?
 - better: measurement of torque to rule out impact of internal losses
 - alternative: use slip (deviation of real rotation from given rotation)

Further possibilities for measurements

- reduction of effective electrical conductivity caused by turbulent fluctuations (**β -effect**)
 - ⇒ **Perm-approach**: global measurement of phase-shift between induced and applied magnetic fields including anisotropy of turbulence (Noskov et al. 2012, Phys.Rev. E 85, 016303)
 - ⇒ **Madison approach**: local measurements of EMF (Rahbarnia et al 2012, Astrophys. J 759, 80)
 - ⇒ important because of large R_m achievable at precession dynamo device (Perm, Madison: $R_m \lesssim 30$)
- **temperature** increase of fluid ⇒ how is energy dissipated, model for viscous dissipation, Joule heating
- 'Seismology' ⇒ calculation of mean circulation from measurements of **propagation of soundwaves**
- **Magnetic field** measurements: coverage, reconstruction, impact of Earth's magnetic field, transformation of reference frames, inverse problems (velocity reconstruction?) ⇒ future topic

References

- Giesecke et al. 2015, *New J. Phys.*, 17 (11), 113044
- Herault et al. 2015, *Phys. Fluids*, 27 (12), 124102
- Stefani et al. 2015, *Magnetohydrodynamics* 51 (2), 275–284
- Giesecke et al. 2018, *Phys.Rev.Lett.* 120 (2), 024502
- Giesecke et al. 2018, *Geophys. Astrophys. Fluid Dyn.*, [10.1080/03091929.2018.1506774](https://doi.org/10.1080/03091929.2018.1506774)
- Herault et al. 2019, *Phys. Rev. Fluids*, 4, 033901